# Clinical applications of optical and optoacoustic imaging techniques in the breast

Wei T. Yang

The University of Texas MD Anderson Cancer Center, Department of Diagnostic Radiology, Division of Diagnostic Imaging, 1515 Holcombe Blvd., Unit 1459, Houston, Texas 77030, USA
Telephone: 713-563-0127, Fax: 713-792-8067, E-mail: wyang@mdanderson.org

## ABSTRACT

Exploitation of the optical properties of tissue to characterize biologic composition has created an era of continuous growth over the past decades for optical imaging. These changes enable the identification of functional abnormalities in conjunction with structural changes of biologic tissue. There is currently a wide array of technologies and applications in development and clinical use. The range of different optical hardware choices has led to systems that utilize optical tissue contrast to address specific clinical needs.

## KEYWORDS

Optical imaging, optoacoustic, ultrasound, diffuse optical spectroscopy, image coregistration, functional imaging, breast cancer, tumor microvasculature, tissue oxygenation

## INTRODUCTION

This manuscript presents an overview of the physical properties of optical and optoacoustic imaging, technological features, and how these technologies address specific clinical needs including, 1) the early detection of breast cancer, 2) the evaluation of the probability of benign vs malignant breast lesions, and 3) the monitoring of neoadjuvant chemotherapy response prior to breast surgery.

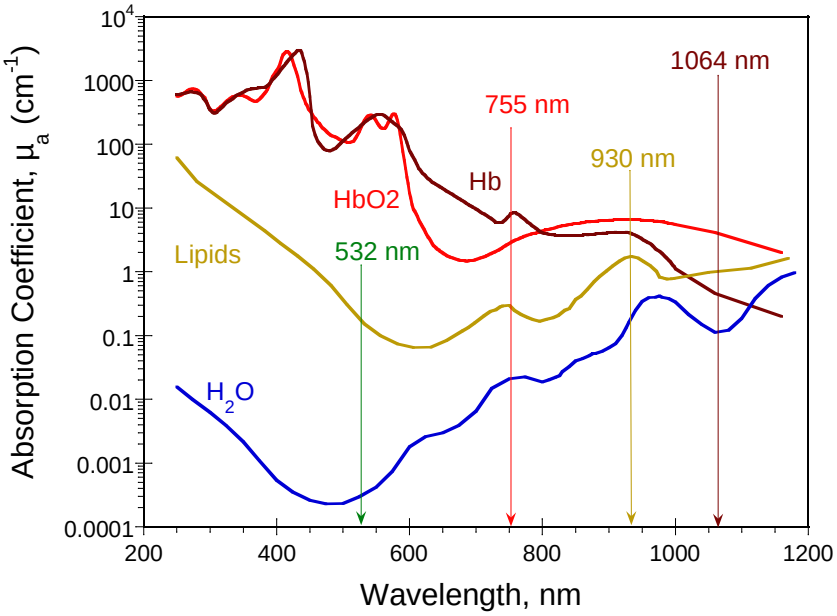


**Figure 1**. Optical absorption spectra of the four major chromophores found in breast tissue.

Medical Imaging 2018: Physics of Medical Imaging, edited by Joseph Y. Lo, Taly Gilat Schmidt, Guang-Hong Chen, Proc. of SPIE Vol. 10573, 105730V
 · doi: 10.1117/12.2300519

**Breast imaging based on optical contrast.**
Optical Imaging comprises a variety of techniques that uses near infrared and visible light, and begins with the excitation of the endogenous and exogenous chromophores by an external source of light. The term chromophore refers to a molecule in biologic tissue under evaluation that is able to interact with light. As presented in Figure 1, the most common chromophores in tissue are: **Hb** (deoxy hemoglobin); Hb not bound to $O_2$ **,** **$O_2$Hb** (oxy-hemoglobin); Hb bound to $O_2$ **,** **$H_2O$** (water), unbound to proteins, **Lipid** [1].

One of the most promising applications of medical imaging based on optical contrast in tissues is in the detection and diagnostics of breast cancer. Breast represents a superficial organ where the remodeled vasculature and changes in the cellular and extracellular tissue secondary to growth of a malignant tumor can be accurately captured by the optical absorption contrast of breast tissue chromophores [2].

**Technological features:**
While the spatial resolution of pure optical imaging methods suffers from significant and random scattering of optical photons in the breast, it is possible to preserve the resolution of an optical image using optoacoustic tomography (OAT), a new breast imaging method that employs ultrasonic transducers to "listen to the sound of light being absorbed" by the breast chromophores [3]. A schematic of OAT illustrates the principles that overcome the problem of optical scattering in breast tissue by detecting ultrasound waves resulting from the optical absorption of near-infrared light (Figure 2).

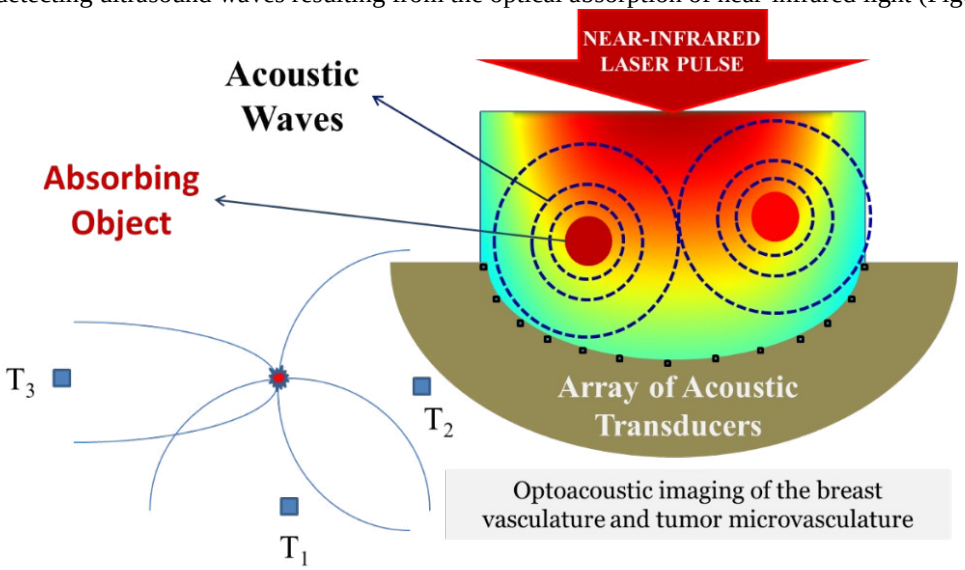


**Figure 2**. Schematic of optoacoustic tomography of the breast and image reconstruction using the principles of triangulation to locate image voxels in 3 dimensions; T1, T2 and T3 represent transducers that detect optoacoustic signals in 3 orthogonal planes [Courtesy Alexander Oraevsky].

There are two internal light absorbing objects (which may represent tumors with specific vascular profiles) within the breast. An arc-shaped array of ultrasonic transducers that detect the optoacoustic signals is placed beneath the breast. A short laser pulse illuminates the entire breast and propagates with attenuation through the depth of the breast tissue while being absorbed preferentially by the light absorbing objects. Ultrasound pulses are launched due to thermal expansion of the objects that absorbed the laser energy prior to expansion (also termed illumination conditions of pressure confinement within the voxels to be resolved on the image). The ultrasound signals (waves) from optically generated sources within the breast (such as tumors with dense angiogenesis related microvasculature) are detected by the array of ultrasonic transducers. Reconstruction of a tomography image is based on the principles of triangulation. The exact location of the voxel on optoacoustic imaging excited by a laser pulse can be determined through the intersection of 3 spherical surfaces with the radius R equal to the time of optoacoustic signal arrival multiplied by the speed of sound. Rigorous methods of image reconstruction for OAT have been developed [4].
Combining grayscale ultrasound with OAT in a dual-modality system is possible because both imaging modalities exploit the detection of ultrasound signals. However, standard ultrasound transducers and analog front end amplifiers designed for medical ultrasound operate using a relatively narrow band of emitted and detected ultrasound frequencies;

the typical bandwidth of standard ultrasound transducers is about 35% around the central frequency, e.g. 8.5MHz ±3.0 MHz. On the other hand, optoacoustic pulses generated through the optical absorption of short laser pulses in biological tissues carry an ultrawide range of ultrasound frequencies ranging from 50 kHz (depending on the characteristic dimensions of the acoustic source) to 10 MHz (higher ultrasound frequencies are strongly absorbed in the breast and cannot penetrate to clinically relevant depths). The primary OAT systems discussed in this review employ ultrawide band ultrasonic transducers and appropriate analog electronics to enable detection of both high frequencies for high spatial resolution and low frequencies for high contrast of volumetric. This combined function of optoacoustic imaging across high and low frequencies permits optimal delineation of lesion morphology and volumetric functional contrast, thereby enabling accurate quantitation of differential tissue composition. Tumor angiogenesis related microvasculature can be accurately represented and the functional parameters of total hemoglobin [tHb] and hemoglobin oxygen saturation [sO2] can be evaluated.

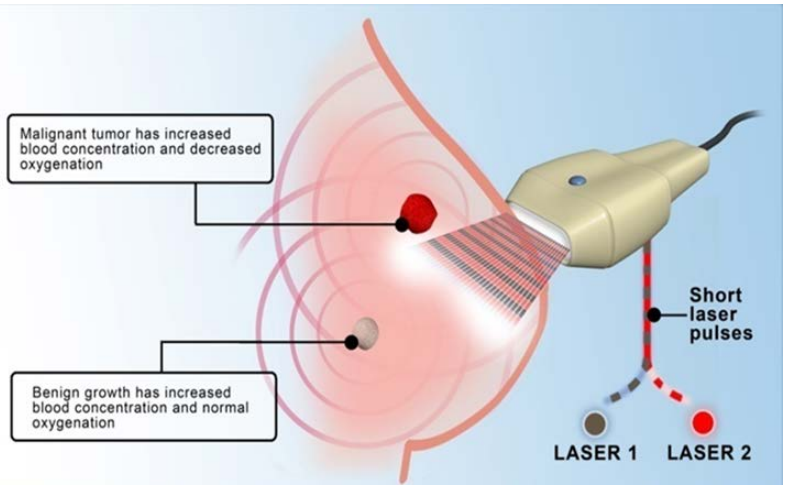


**Figure 3**. Schematic diagram of diagnostic imaging of breast cancer using functional optoacoustic imaging coregistered with B-mode ultrasound [Courtesy Seno Medical Instruments, San Antonio, TX].

**Clinical applications:**

The major unmet needs that continue to challenge the breast imaging community include the following: (1) Screening for the early detection of breast cancer remains controversial with increasing debate around the opportunity to create customized screening regimens for women who are at high risk for developing breast cancer, and to seek less aggressive screening regimens for women who are at low risk for the development of breast cancer or who develop biologically less aggressive breast cancer that is unlikely to metastasize or lead to death, (2) Accurate differentiation of benign from malignant breast lesions to reduce the cost and morbidity of unnecessary benign biopsies, (3) Effective monitoring of neoadjuvant response to chemotherapy to a) enable the early identification of nonresponders and allow for enrollment in adaptive therapeutic clinical trials, and b) enable accurate identification of complete histopathologic responders to enable them to consider enrollment in alternate nonsurgical adjuvant therapeutic clinical trials.

**1) Early detection of breast cancer and 2) Accurate characterization of benign from malignant breast lesions**

A recent publication describes the preliminary findings from a prospective multisite study of 2105 women that compared Breast Imaging Reporting and Data System (BI-RADS) categories for benign and malignant breast masses using optoacoustic ultrasound versus ultrasound alone [5]. This study included BI-RADS 3, 4, and 5 masses with histopathologic correlation, and/or a 12 month follow-up for BI-RADS 3 masses. Independent reader review was performed and a BI-RADS category and probability of malignancy was assigned to each mass before and after scoring of optoacoustic features. The benign and malignant mass upgrade and downgrade rates, positive and negative predictive values, and positive and negative likelihood ratios were compared. The 2D handheld optoacoustic system used in this study acquires a sequence of three 2D images with video frame rate that include: (i) gray scale ultrasound image, (ii) optoacoustic image with illumination by laser pulses at 1064 nm wavelength, (iii) optoacoustic image with illumination by laser pulses at 757 nm wavelength (Figure 3). Because all 3 images are coregistered in space and time, the optoacoustic images can be converted into the functional images of [tHb] and [sO2]; each functional image is then overlaid on the gray scale anatomical image with breast morphology. Since malignant and aggressively growing breast

lesions typically have enhanced angiogenesis microvasculature and blood in the tumor is typically hypoxic [6], these functional optoacoustic ultrasound images permit improved differentiation of malignant from benign tumors when compared with the diagnostic specificity of ultrasound alone. The findings from this study showed that optoacoustic functional imaging increases the specificity of breast mass assessment by approximately 2 fold when compared to ultrasound alone [5]. Optoacoustic ultrasound downgraded 40.8% of benign mass reads, with a specificity of 43% for optoacoustic ultrasound versus 28.1 % for internal gray scale ultrasound of the device alone [5]. Figures 4 and 5 show panels of 4 images: gray scale ultrasound (upper left), [tHb] overlaid with ultrasound where yellow pixels show brightness above medium level (lower left), [sO2] images overlaid with ultrasound on the right (upper and lower) are thresholded to show blood oxygenation only, where red pixels show hypoxia and green pixels show normoxia; the upper right images are thresholded to demonstrate blood oxygenation in the region corresponding to the yellow optoacoustic pixels at the lower left.

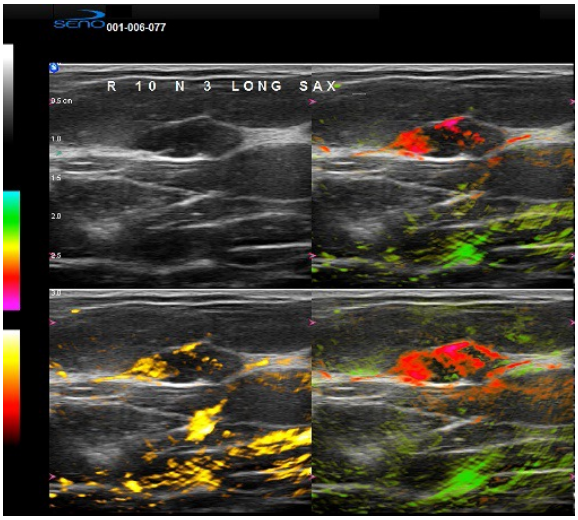


**Figure 4**. 58-year-old female called back for abnormal mammogram. Gray scale ultrasound shows an oval circumscribed hypoechoic mass (top left), categorized as BI-RADS 3. Optoacoustic ultrasound demonstrates significant increased signal in the periphery and center of the mass (bottom left) reflecting increased tHB. Top and bottom right images show increased red pixels reflecting deoxygenated HB (hypoxia), leading to an upgrade to BI-RADS 4 (suspicious for malignancy). Histopathology showed DCIS, nuclear grade 2, hormone positive; HER2 not obtained [Courtesy Seno Medical Instruments, San Antonio, TX].

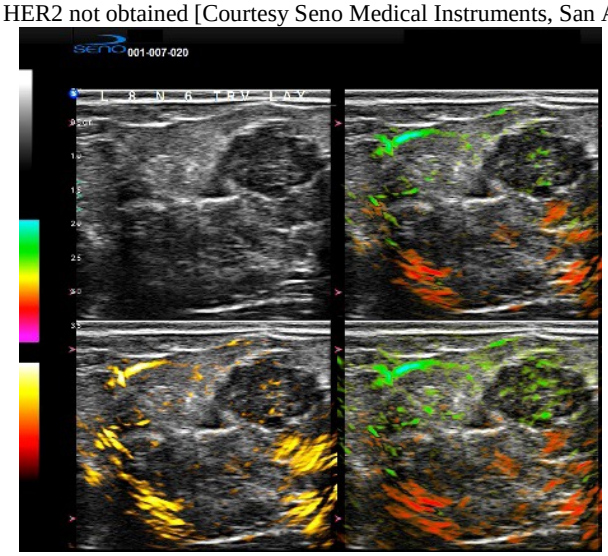


**Figure 5**. 82-year-old female presenting with palpable abnormality. Gray scale ultrasound (top left) shows a lobular slightly microlobulated hypoechoic mass, categorized as BI-RADS 4b (suspicious for malignancy). Optoacoustic ultrasound shows minimal internal signals (bottom left) reflecting decreased tHB, and sparse internal green pixels (top and bottom right) reflecting normoxic vascularity, leading to a downgrade to BI-RADS 3. Histology showed benign fibroadenoma [Courtesy Seno Medical Instruments, San Antonio, TX].

The advantages of 2D optoacoustic imaging include simple user interface with hand-held probes, natural co-registration with a single ultrasound probe and electronics, combined optical and acoustic contrast that allows tissue anatomy correlation with tissue function and molecular content. Further, 2D optoacoustic imaging delivers real-time video rate images, 2D slices are easy to display without the need for post-processing, and the visual display is familiar for end users including ultrasonographers, radiologists, and surgeons. Limitations of the 2D system includes the inability to accurately quantitate functional images with hand-held probes, the inability to display background breast morphology relative to the tumor, and the inability to perform automated screening of an entire breast. Recognition of the inherent limitations of the hand-held probe based systems led to the development of the full view 3D systems. A leading 3D dual-modality system is the Laser Optoacoustic Ultrasonic Imaging System Assembly (LOUISA-3D) developed by TomoWave Laboratories (Houston, TX) and currently in preparation for clinical feasibility studies at the University of Texas MD Anderson Cancer Center (Houston, TX).

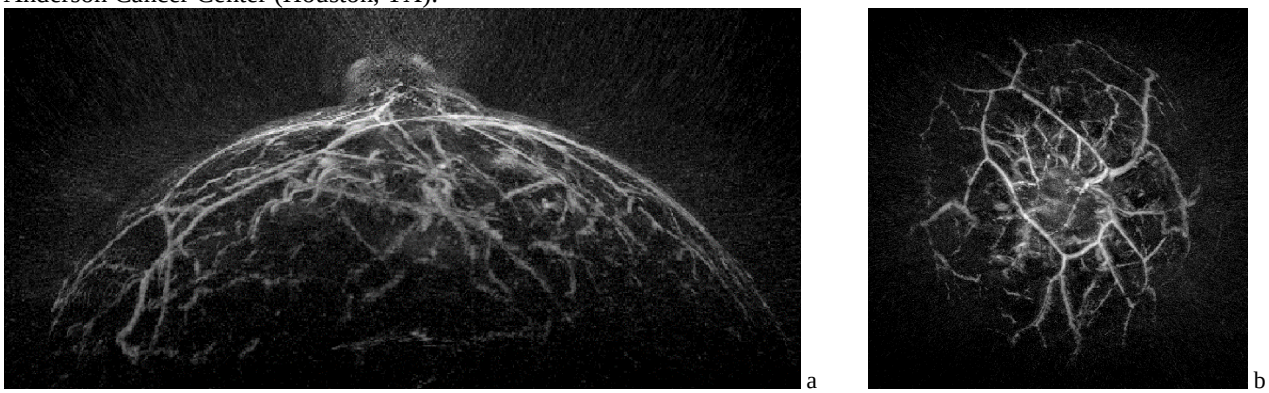


**Figure 6**. Maximum intensity projection LOUISA-3D optoacoustic images of the breast obtained with a 3D system: (a) sagittal projection and (b) coronal projection.

Figure 6 depicts maximum intensity projections (sagittal and coronal) of a 3D optoacoustic image of a normal breast. This image displays breast vasculature from the nipple to the chest wall with an average resolution of approximately 350 microns in 3 dimensions throughout the breast volume. Figure 7 illustrates a sagittal image through a 3D optoacoustic image coregistered with 2D ultrasound gray scale morphology in a normal breast. In order to achieve high contrast and high resolution, the imaging module of this system contains an 85 degree arc-shaped linear array of ultrasonic transducers (with ultrawide bandwidth of 50 kHz to 8 MHz) rotating round the breast that is illuminated by Alexandrite laser pulses (Light Age, Somerset, NJ) delivered through a fiberoptic system independently rotating round the breast [7]. The medical grade Alexandrite laser provides 50-ns pulses at up to 20 Hz repetition rate with energy of 650 mJ at two toggling wavelengths, 797 nm and 757 nm [8]. While the wavelength of 797 nm allows visualization of all vasculature independently on [sO2], the wavelength of 757 nm permits high contrast visualization of the tumor angiogenesis with hypoxic blood.

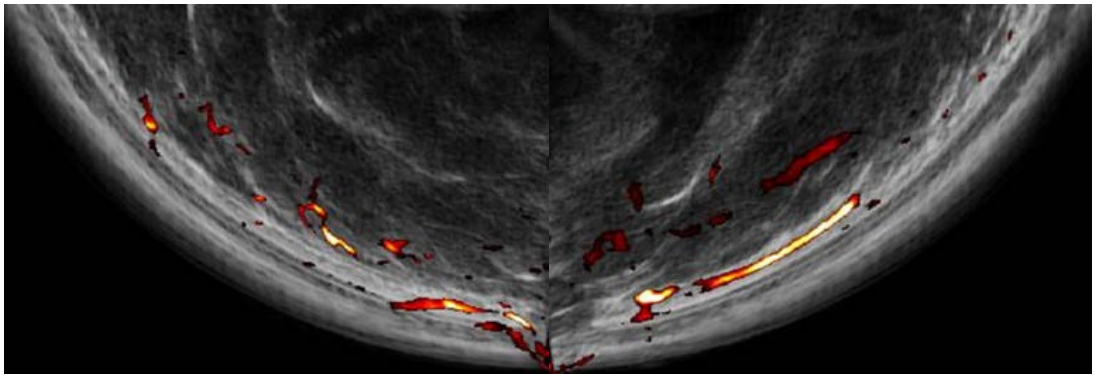

**Figure 7**. Sagittal LOUISA-3D optoacoustic image of the normal breast coregistered with 2D ultrasound breast morphology.

The duration of the full view scan is about 6 min for 20 illumination steps of toggling wavelengths and 320 angular views of 96-channel transducer array resulting in the detection of optoacoustic signals by 30,720 virtual transducers

positioned on a hemispherical surface. Rigorous reconstruction in spherical coordinates from around hemispherical volume of the breast generates a 3D image with over 100 million voxels in less than 4 minutes using NVidia GPU card with 2560 parallel cores.

In summary, 3D combined optoacoustic and ultrasonic imaging systems in one assembly allows coregistration of functional and anatomical information in three dimensions. 3D OAT systems represent a potential hybrid imaging modality with sufficient resolution and contrast for functional quantitation, and offers the possibility of automated examinations for whole breast screening. The potential clinical application in screening for breast cancer may provide value in populations where MRI screening of women with high risk or dense breasts is problematic as a function of cost, and access.

**3) Monitoring the effects of neoadjuvant chemotherapy prior to breast surgery**

Effective monitoring of neoadjuvant response to chemotherapy will enable the early identification of nonresponders to allow enrollment in adaptive therapeutic clinical trials, and accurate identification of complete histopathologic responders will enable enrollment in clinical trials that consider alternate nonsurgical adjuvant therapeutic clinical trials. The application of advanced MRI techniques such as volumetric measurements, MRI tumor morphology phenotype, peak enhancement kinetics, radiogenomics, DWI, and textural analysis to assess response in breast cancer patients receiving neoadjuvant chemotherapy has been aggressively investigated in the past decade [9-26]. While promising results have been reported with breast MRI, efforts are ongoing to develop a simple, reproducible, inexpensive functional imaging tool that can accurately quantitate response to neoadjuvant therapy early in the treatment cycle.

Diffuse Optical Spectroscopic Imaging (DOSI) is a handheld device that captures measureable differences in optical contrast based on differences in the 2 states of hemoglobin. In normal conditions, the ratio between oxy- and deoxyhemoglobin is highly conserved. This ratio is changed for malignant tumors. The prospective multicenter ACRIN 6691 trial was designed to evaluate whether changes at mid-point of therapy relative to baseline using a DOSI-derived imaging endpoint (described as the tissue optical index [TOI]) is able to predict for eventual pathologic complete response (pCR) [27]. DOSI systems were constructed at the University of California, Irvine and delivered to 6 major institutions where 60 subjects with newly diagnosed primary invasive breast cancer were enrolled. Handheld bedside DOSI images were obtained and the tissue concentrations of deoxyhemoglobin, oxyhemoglobin, water, lipid, and the TOI was acquired of both breasts at baseline, 1 week, mid-point of therapy, and at the end of therapy [27]. Data derived from 34 evaluable patients validated high instrument precision for quantitative longitudinal studies across multiple sites, and demonstrated that the $\%TOI_{TN}$ AUC was 0.60 (95% CI, 0.39-0.81) using pCR as the reference standard and ROC curve methodology [27]. These preliminary findings suggest that combined baseline functional properties and dynamic optical-based tissue response characteristics are promising for the prediction of therapeutic outcome in breast cancer patients.

## ACKNOWLEDGEMENT

This research was supported in part by the National Cancer Institute, NIH grant R01167446 and by Seno Medical Company, San Antonio, Texas.

This research was supported by the American College of Radiology Imaging Network, ACRIN, which receives funding from the National Cancer Institute (NCI) through the grants U01 CA079778 and U01 CA080098 (clinical trial information: NCT01217385), the National Institute of Biomedical Imaging and Bioengineering (P41EB015890), the National Cancer Institute (R01CA142989, U54CA136400), and the Chao Family Comprehensive Cancer Center (P30CA62203), and programmatic support from the Arnold and Mabel Beckman Foundation.

## REFERENCES

[1] Cerussi, A.E., Shah, N.S., Hsiang, D., Durkin, A., Butler, J.A.; Tromberg, B.J., "In vivo absorption, scattering, and physiologic properties of 58 malignant breast tumors determined by broadband diffuse optical spectroscopy", J. Biomed Optics, 11(4), 044005 (2006). doi:10.1117/1.2337546

[2] Herranz, M., Ruibal, A., "Optical imaging in breast cancer diagnosis: The next evolution", J Oncol, 863747 (2012**).**

[3] Oraevsky, A.A., [Biomedical Photonics Handbook], CRC Press, Boca Raton, Chapter 21, 715-757 (2014).

[4] Wang, K., Su, R., Oraevsky, A.A., Anastasio, M.A., "Investigation of iterative image reconstruction in three-dimensional optoacoustic tomography", *Phys. Med. Biol*., 57 5399-5423 (2012), DOI: 10.1088/0031-9155/57/17/5399

[5] Neuschler, E.I., Butler, R., Young, C.A., Barke, L.D., Bertrand, M.L., Böhm-Vélez, M., Destounis, S., Donlan, P., Grobmyer, S.R., Katzen, J., Kist, K.A., Lavin, P.T., Makariou, E.V., Parris, T.M., Schilling, K.J., Tucker, F.L., Dogan, B.E., "Imaging to diagnose benign and malignant breast masses: A new evaluation tool for radiologists", Radiology, 286 (2018). https://doi.org/10.1148/radiol.2017172228
[6] Chance, B., Nioka, S., Zhang, J., Conant, E.F., Hwang, E., Briest, S., Orel, S.G., Schnall, M.D., Czerniecki, B.J.,"Breast cancer detection based on incremental biochemical and physiological properties of breast cancers: A six-year, two-site study", *Acad Radiol* 12, 925–933 (2005).
[7] Oraevsky, A.A., Su, R., Nguyen, H., Moore, J., Lou, Y., Bhadra, S., Forte, L., Anastasio, M., Yang, W.T., "Full-View 3D imaging system for functional and anatomical screening of the breast", *Proc. SPIE* **10494**, 248 (2018).
[8] Klosner, M., Chan, G., Wu, C., Heller, D.F., Su, R., Ermilov, S.A., Brecht, H.P., Ivanov, V., Talole, P., Lou, Y., Anastasio, M., Oraevsky, A.A., "Advanced Laser System for 3D Optoacoustic Tomography of the Breast", Proc. SPIE 9708, 97085B (2016), doi: 10.1117/12.2209398.
[9] American College of Radiology Imaging Network (ACRIN) 6698, "Diffusion weighted MR imaging biomarkers for assessment of breast cancer response to neoadjuvant treatment: A sub- study of the I-SPY 2 TRIAL (Investigation of Serial Studies to Predict Your Therapeutic Response with Imaging and molecular Analysis)" ACRIN, (2012). https://www.acrin.org/TabID/825/Default.aspx. Accessed January 16, 2017.
[10] Hylton, N.M., Gatsonis, C.A., Rosen, M.A., et al., ACRIN 6657 Trial Team and I-SPY 1 TRIAL Investigators,"Neoadjuvant chemotherapy for breast cancer: Functional tumor volume by MR imaging predicts recurrence-free survival-results from the ACRIN 6657/CALGB 150007 I- SPY 1 TRIAL", Radiology, 279(1), 44-55 (2016).
[11] Bae, M.S., Shin, S.U., Ryu, H.S., et al, "Pretreatment MR imaging features of triple-negative breast cancer: Association with response to neoadjuvant chemotherapy and recurrence-free survival", Radiology, 281(2), 392-400 (2016).
[12] Esserman, L., Kaplan, E., Partridge, S., et al., "MRI phenotype is associated with response to doxorubicin and cyclophosphamide neoadjuvant chemotherapy in stage III breast cancer", Ann Surg Oncol, 8(6), 549-559 (2001).
[13] Kim, T.H., Kang, DK, Yim, H, et al., "Magnetic resonance imaging patterns of tumor regression after neoadjuvant chemotherapy in breast cancer patients: correlation with pathological response grading system based on tumor cellularity", J Comput Assist Tomogr, 36(2), 200-206 (2012).
[14] Marinovich, M.L., Houssami, N., Macaskill, P., et al. "Meta-analysis of magnetic resonance imaging in detecting residual breast cancer after neoadjuvant therapy", J Natl Cancer Inst., 105(5), 321-333 (2013).
[15] Londero, V., Bazzocchi, M., Del Frate, C., et al., "Locally advanced breast cancer: Comparison of mammography, sonography and MR imaging in evaluation of residual disease in women receiving neoadjuvant chemotherapy", Eur. Radiol., 14(8), 1371-1379 (2004).
[16] De Los Santos, J.F., Cantor, A., Amos, K.D., et al., "Magnetic resonance imaging as a predictor of pathologic response in patients treated with neoadjuvant systemic treatment for operable breast cancer. Translational Breast Cancer Research Consortium trial 017", Cancer, 119(10), 1776-1783 (2013).
[17] Bouzón, A., Acea, B., Soler, R., et al., "Diagnostic accuracy of MRI to evaluate tumour response and residual tumour size after neoadjuvant chemotherapy in breast cancer patients", Radiol. Oncol., 50(1), 739 (2016).
[18] Mukhtar, R.A., Yau, C., Rosen, M., Tandon, V.J., I-SPY 1 TRIAL and ACRIN 6657 Investigators, Hylton, N., Esserman, L.J., "Clinically meaningful tumor reduction rates vary by prechemotherapy MRI phenotype and tumor subtype in the I-SPY 1 TRIAL (CALGB 150007/150012; ACRIN 6657)", Ann. Surg. Oncol., 20(12), 3823-3830 (2013).
[19] Partridge, S.C., Nissan, N., Rahbar, H., et al., "Diffusion-weighted breast MRI: Clinical applications and emerging techniques", J Magn. Reson. Imaging, 45(2), 337-355 (2017).
[20] Chen, X., Li, W.L., Zhang, Y.L., et al., "Meta-analysis of quantitative diffusion-weighted MR imaging in the differential diagnosis of breast lesions", BMC Cancer, 10, 693 (2010).
[21] Kim, S.H., Cha, E.S., Kim, H.S., et al., "Diffusion-weighted imaging of breast cancer: correlation of the apparent diffusion coefficient value with prognostic factors", J. Magn. Reson. Imaging, 30(3), 615-620 (2009).
[22] Kamitani, T., Matsuo, Y., Yabuuchi, H., et al., "Correlations between apparent diffusion coefficient values and prognostic factors of breast cancer", Magn. Reson. Med. Sci., 12(3), 193-199 (2013).
[23] Mazurowski, M.A., Zhang, J., Grimm, L.J., et al., "Radiogenomic analysis of breast cancer: luminal B molecular subtype is associated with enhancement dynamics at MR imaging", Radiology, 273(2), 365-372 (2014).
[24] Sutton, E.J., Oh, J.H., Dashevsky, B.Z., et al., "Breast cancer subtype intertumor heterogeneity: MRI-based features predict results of a genomic assay", J. Magn. Reson. Imaging, 42(5), 1398-1406 (2015).
[25] Ahmed, A., Gibbs, P., Pickles, M., Turnbull, L., "Texture analysis in assessment and prediction of chemotherapy response in breast cancer", J. Magn. Reson. Imaging, 38(1), 89-101 (2013).

[26] Park, S.H., Moon, W.K., Cho, N., et al., “Diffusion-weighted MR imaging: pretreatment prediction of response to neoadjuvant chemotherapy in patients with breast cancer”, Radiology, 257(1), 56-63 (2010).
[27] Tromberg, B.J., Zhang, Z., Leproux, A., O’Sullivan, T.D., Cerussi, A.E., Carpenter, P.M., Mehta, R.S., Roblyer, D., Yang, W.T., Paulsen, K.D., Pogue, B.W., Jiang, S., Kaufman, P.A., Yodh, A.G., Chung, S.H., Schnall, M., Snyder, B.S., Hylton, N., Boas, D.A., Carp, S.A., Isakoff, S.J., Mankoff D., on behalf of the ACRIN 6691 investigators, “Predicting responses to neoadjuvant chemotherapy in breast cancer: ACRIN 6691 trial of diffuse optical spectroscopic imaging,” Cancer Res., 76 (20) 5933-5944 (2016), **DOI:** 10.1158/0008-5472.CAN-16-0346